EPSC Abstracts
Vol. 11, EPSC2017-660-1, 2017
European Planetary Science Congress 2017


# Correlation of Radar and Visible Data of Mars' North Polar Layered Deposits

P. Becerra (1), I. Smith (2), D. Nunes (3), M.M. Sori (4), Y. Brouet (1), N. Thomas (1), and L. Guallini (1)
(1) Physikalisches Institut, Universität Bern, Switzerland (2) Planetary Science Institute, Tucson, AZ, USA. (3) Jet Propulsion Laboratory, Pasadena, California, USA (4) University of Arizona, Tucson, AZ, USA.

## Abstract

We attempt to correlate two major datasets currently used to explore Mars' Polar Layered Deposits: Visible imagery and stereo-topography from HiRISE and sub-surface radar from SHARAD. The resulting stratigraphic columns can constrain formation models for the deposits and will be used to explore their connection to Mars' Amazonian climate evolution.

## 1. Introduction

A long-standing problem in Mars Polar Science is the interpretation of the stratigraphic record preserved in Mars' icy North Polar Layered Deposits (NPLD) [1] (Fig. 1a), whose accumulation patterns of ice and dust have long been associated with recent climatic changes due to temporal variations in the planet's astronomical parameters [2,3]. The internal layering of the NPLD is visible from orbit in exposures within a series of spiraling troughs that dissect the NPLD dome (Fig. 1a,b). Studies have relied on remote images of these troughs to map the stratigraphy [5-9] and search for a connection between NPLD accumulation and astronomical forcing [10-13]. Sub-surface sensing radar sounding has also proved invaluable in observing the internal structure of the deposits. The Shallow Radar (SHARAD) instrument [14] detects changes in dielectric properties with depth. As these vary for layers with different amounts of dust contamination, layering is observed in the radar data as "reflector" surfaces [15].

The optical and radar-based stratigraphies have predominantly been studied in isolation. In terrestrial climate science [17], orbital climate forcing was ultimately confirmed by the correlation of sedimentary, geochemical and paleo-magnetic records, suggesting that integration of datasets is necessary to build a complete climate record for the NPLD. In general, both radar and optical layers are assumed to result from varying amounts of silicic impurities in water ice [19]. Christian et al. [18] attempted the first quantitative correlation and found a general agreement between properties of radar reflectors and visible layers. This provided evidence that the same physical quantity (potentially dust fraction) controls the formation of both sub-surface radar reflectors and protruding strata. However, they were unable to achieve a unique correlation between one radar reflector and one visible layer or packet.

Here, we present our approach to this correlation by modeling the SHARAD propagation through permittivity profiles constrained by HiRISE-derived topographic profiles [9]. The objective is to combine the information from both datasets to obtain a dust-fraction-based NPLD stratigraphic profile at the finest resolution possible. These profiles can constrain orbitally-forced climate-accumulation models [20,21], thereby illuminating the connection between orbital history, climate, and polar accumulation during the formation of the NPLD.

## 2. Methods

The goal of the data integration is to obtain dust content vs. depth profiles that can be directly compared to the output of layer accumulation models. Our approach: (1) Model the radar wave propagation through synthetic permittivity profiles constrained by a relationship between the HiRISE-derived topographic expression of the layers, and permittivity (ε). (2) Correlate these profiles to real SHARAD data using spectral analysis and pattern-matching algorithms. This correlation results in HiRISE-SHARAD stratigraphic profiles of ε, which can be transformed to fractional dust-content [23] and thereby be used to constrain accumulation models.

We use the radar-propagation model of [19] and the HiRISE topography products of [9]. The layered medium through which we propagate the model radar wave is a ε profile constrained by the protrusion profiles of [9], which measure topographic expression of layers at the resolution of HiRISE Digital Terrain Models (DTMs) by calculating how much a layer deviates from an average linear fit to the trough slope [9] (e.g. fig. 2a,b).

## 3. Preliminary Results

Since we know that dust content affects the dielectric response of subsurface ice, and we assume that it affects protrusion [9,21] we make the change in ε with depth of the model profile depend on the

layer protrusion. The average fractional dust content within the NPLD is <5% [24], corresponding to an average ε = 3.1. Individual layers can have higher or lower values [25]. We search for an empirical model that relates protrusion to ε by varying the ε of layers between that of pure ice (3.0–3.15) and the highest values observed at the NPLD by [24] (~3.8), although this will vary to account for updated maximum values [25], and the possibility of high porosity [26]. The model radar profiles in Fig. 2c simulate the SHARAD pulse through a medium constrained by selected protruding layers from the profile at site N0 (known as "Marker Beds" [5]; Fig. 1a, 2b) corresponding to a depth of ~ 250 m, which were assigned a ε of 3.5 and a background ε of 3.15. Fig. 2c shows that thick protrusion peaks (>15 m) are resolvable, while thinner layers could be difficult to distinguish. A comparison with the observed radargram at site N0 (fig. 2d) shows that between 2.5 and 5 μs (~200 – 400 m in depth), there is a similar number of reflections in the observation (5-6) and the model (6-7), demonstrating that they are comparable.

# 4. Future Work

Our preliminary investigations have promising results. We will extend this study and generate synthetic radar profiles based on different empirical ε–protrusion relations at each site shown in fig. 1a. We will select 2–10 SHARAD observations to calculate average depth vs. power profiles (e.g. Fig. 2d) at locations near each trough wall, so that each site has a representative radar and protrusion profile. To correlate the synthetic radar profiles to SHARAD data, we will use two complementary methods: Wavelet analysis [13,27] and dynamic-time warping [9,28]. The first will estimate similarities between profiles by comparing their spectral properties, and the second will perform the direct correlation of profiles to select the best ε–protrusion empirical model. Further work involves comparing the integrated stratigraphy with formation models controlled by orbital cycles [e.g. 21].

# 5. Figures

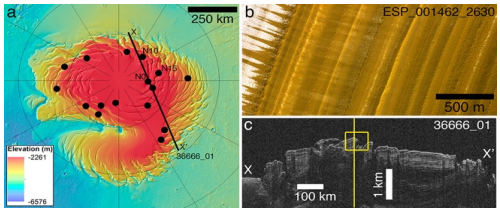


Figure 1. (a) Topographic map of the NPLD. Dots = locations of study sites and HiRISE DTMs from [9]. The line is the ground track of the SHARAD radargram shown in (c). (b) HiRISE image of exposed layers in an NPLD trough. (c) SHARAD radargram (X-X' in 1a). The square marks the approximate location of site N0. The line shows the position of the profile of Fig. 2d.

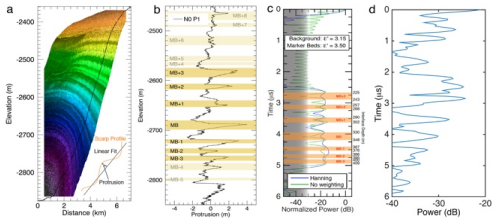


Figure 2. (a) HiRISE DTM and topographic profile of site N0. Inset is a schematic of the protrusion calculation [9]. (b) Protrusion profile of site N0. "Marker Beds" (MB) correlated to the stratigraphy of [7] are shown (c) Example synthetic radar profile produced by wave propagation through marker beds of 2b using a simple compressed pulse (green), and one weighted by a Hanning window (blue) [19]. (d) SHARAD radar profile near site N0. Delay times and power for both (c) and (d) are referenced to the first arrival of the surface reflection.


## Acknowledgements

Part of this work is funded by the Swiss National Centre of Competence in Research (NCCR) PlanetS.


## References


[1] Clifford, et al. *Icarus* 225 (2013) [2] Cutts *JGR* 78 (1973) [3] Cutts, et al. *Science* 194 (1976) [4] McEwen et al. *JGR* 112 (2007) [5] Fishbaugh et al. *JGR* 111 (2006) [6] Tanaka et al. *Icarus* 196 (2008) [7] Fishbaugh et al. *GRL* 37 (2010) [8] Limaye et al. *JGR* 117 (2012) [9] Becerra et al. *JGR* 121 (2016) [10] Laskar et al. *Nature* 419 (2002) [11] Milkovich and Head, *JGR* 110 (2005) [12] Perron and Huybers, *Geology* 37 (2009) [13] Becerra et al. *GRL* 44 (2017) [14] Seu et al. *JGR* 112 (2007) [15] Putzig et al. *Icarus* 204 (2009) [16] Smith et al. *Science* 352 (2016) [17] Imbrie, *Icarus* 50 (1982) [18] Christian, et al. *Icarus* 226 (2013). [19] Nunes & Phillips, *JGR* 111 (2006) [20] Levrard et al. JGR 112 (2007) [21] Hvidberg et al. *Icarus* 221 (2012) [23] Stillman, et al. *J.Phys.Chem.* 114 (2010) [24] Grima, et al. *GRL* 36 (2009) [25] Lalich and Holt, *GRL* 44 (2017) [26] Bramson et al. *GRL* 42 (2017) [27] Torrence and Compo, *Bull. Am. Met. Soc.* 79 (1998) [28] Sori et al. *Icarus* 235 (2014).